Title: Does assigning intentions to others involve visual motion processing?

Marius Görner[†1,2,3], Masih Shafiei[†1,2,3], and Peter Thier[*1,4]

[1] Hertie Institute for Clinical Brain Research, Cognitive Neurology, Tübingen, Germany

[2] GTC of Neuroscience, Tübingen, Germany

[3] IMPRS for Cognitive and Systems Neuroscience, Tübingen, Germany

[4] Werner Reichardt Centre for Integrative Neuroscience, Tübingen University, Tübingen, Germany

*Corresponding author: Peter Thier, Hoppe-Seyler-Str. 27, 72076 Tübingen, Germany. (e-mail: thier@uni-tuebingen.de).

[†]M.G. and M.S. contributed equally to this work

Keywords:

Gaze following, intentional binding, implied motion, motion adaptation, social attention

Abstract

We use others' gaze to identify their object of attention. Guterstam and colleagues suggested that the capability to link the gaze of observed persons to their object of interest is mediated by an imaginary "gaze beam" that emanates from the others' eyes and moves through space. The central tenet of this hypothesis is that the gaze beam recruits the visual motion processing system. Görner *et al*. argued that the experimental evidence supports not only this "gaze beam hypothesis" but also a different interpretation, namely the beholder´s understanding that the other displays a particular object-related intention. We refer to this as "intentional binding hypothesis". This assignment of an intention may involve the prediction of an upcoming movement of the observed person engaging the same system. To critically compare the explanatory power of the two hypotheses, we aim to replicate and extend the original psychophysical study by Guterstam et al. to test the alternative hypothesis.

Introduction

A fundamental aspect of our social life is to identify the interests of our peers. The other's gaze directed at objects of interest is a particularly rich source of expedient information. But how we might link others' gaze to their object of interest remains unknown. In an attempt to find an answer, Guterstam et al. ran a series of studies[1–4]. A promising finding, reported in the first publication[1] was that the presence of a person's gaze affected the judgement of the critical angle at which a vertical bar toppled over. They interpreted this observation as if a directed "force carrying beam", emanating from the eyes pushes on the object[1]. In subsequent studies, they presented evidence that this imaginary beam had motion-like properties[2,3]. This conclusion was suggested by the fact that observing a static image of a face gazing at a tree (*face* stimulus, Fig. 1) influenced reaction times (RT) when reporting the motion direction of a subsequently presented random dot motion stimulus (RDMS)[2]. RTs in the incongruent condition, where the direction of RDMS was opposite to the gaze direction in the preceding cue image, were faster than in the congruent condition (face effect)[2]. A similar differential effect on RTs characterizes the standard motion adaptation effect[5–7], in which an adapting motion pattern precedes judgements on motion direction. Motion adaption may also be induced by static images lacking real motion but implying motion such as a photo of a running animal[6,7]. Against this backdrop they concluded that also the other´s gaze, depicted in the static image directed towards the tree would imply motion and consequently induce motion adaption. We refer to this idea as the *gaze-beam hypothesis* or GBH. The neural underpinning of this concept was investigated in an fMRI study in which Guterstam and colleagues found that the visual motion areas were indeed activated when the observer was exposed to another person's gaze[3] as predicted by the GBH.

In a commentary, Görner and co-workers argued against the GBH by pointing out conceptual limitations inherent in this interpretation and suggested an alternative[8]. They proposed that the observer's expectation of motion of the agent and/or the object depicted in the image could be the cause of the activation of visual motion processing areas (MT+). They reasoned that the observer will inevitably perceive the agent in the image as an intentional being about to manipulate the object, associated with the expectation of motion[9,10]. Such predictions of the other´s intention are needed in order to prepare proper reactions and, more generally, to shape the observer's own behaviour which is fundamental to successful social interactions[11]. In fact, the idea that the expectation of movement may activate visual motion processing areas is well supported by previous work on the effects of imagined, predicted and remembered motion[9,10,12–14]. Here, we refer to the idea that the attribution of intentions may evoke percepts of motion as the *intentional binding hypothesis* (IBH). Importantly, unlike the GBH, the IBH predicts that assigning intention to others recruits MT+ if the semantics of the scene suggests an object directed intention even though the agent depicted in an image does not yet attend to the object.

In the current study, we will first repeat the original experiment of Guterstam and colleagues[2] using the two main stimuli, a face looking towards a tree or, alternatively, gazing in the opposite direction (*mirrored-face* stimulus, Fig. 1). In contrast to the former, Guterstam and colleagues found that the latter did not cause motion adaptation. Secondly, we will test the IBH by investigating whether the motion adaptation effect is elicited by the rendition of a scene that implies object-oriented intentions of a person. This is implemented through an image that features a forest-worker standing a few steps away from a single tree and pulling the starter rope of a chainsaw to fell it (*person-with-chainsaw* or *PWC*; Fig. 1). A key feature is that the worker 's eyes are obscured behind the visor of a cap and that the head is oriented downwards towards the chainsaw rather than to the tree, while the chainsaw is pointing to the tree. We assume that the compelling interpretation of this image is that the person intends to move towards the tree to fell it while his immediate attention is directed towards the chainsaw. Thereby, the *PWC* condition allows to distinguish intention (to cut the tree) from visual attention (devoted to the chainsaw). To test whether the orientation of the chainsaw matters, we will include a mirrored version of the *PWC* stimulus, in which the tool points to the opposite side. Further, as Guterstam et al. proposed that the gaze-effect is based on perceiving the stimulus as implied motion[2,3], we will add a dedicated control of implied motion to the experiment by resorting to a static image of horses running to the left or right. Lastly, to test the ability of our experimental setup to reveal the motion after-effect elicited by real motion, we will recreate the moving grating stimulus used by Guterstam et al. in their original study[2].

If the judgment of motion-direction in the *face, PWC*, and the *horses* conditions yields faster RTs in the incongruent relative to the congruent condition ($\mathrm{RT}_{ic} < \mathrm{RT}_c$) then we will interpret this effect as motion adaptation caused by implied motion (Q1, Q3, and Q5 in Table 1). However, if we find the inverse effect ($\mathrm{RT}_{ic} > \mathrm{RT}_c$), then this would suggest response priming[15,16] – a facilitation of the motor response because of the agreement of directional information in the stimulus and the direction of the response. Depending on the respective outcome in the mirrored conditions the effects are orientation dependent or not (Q2 and Q4 in Table 1). Note that the direction of the stimulus image is always defined as towards the tree. Finally, the grating stimulus is intended to validate our experimental setup; we expect $\mathrm{RT}_{ic} < \mathrm{RT}_c$ (Q6, Table 1). The above specified hypotheses will be tested for each participant individually. To ensure that individual results are reliable, we will use Bayesian analysis methods and collect data from each participant until the calculated Bayes Factors are ≥ 10 in favour of or against the respective null hypothesis (Table 1).

Assigning intentions to others arguably depends on one's own experiences and preferences which might result in qualitatively different experimental outcomes across subjects ($\Delta\mu_{RT} > 0$, $\Delta\mu_{RT} = 0$, or $\Delta\mu_{RT} < 0$, where $\Delta\mu_{RT} = \Delta\mu_{RT_{ic}} - \Delta\mu_{RT_{c}}$). Therefore, to nonetheless obtain meaningful results at the population level, we will analyse the distribution of individual experimental outcomes rather than calculating simple population average RTs. Our understanding is that Guterstam et al. consider the GBH to be a fundamental property of human social perception which is why we expect to find the respective effects in the majority of our subjects. Thus, support for the GBH requires that the following four conditions will be met by our population of participants (Q7). First, (A1) in the *face* condition the number of participants with an effect of $\Delta\mu_{RT} < 0$ must be larger than expected by chance (= $1/3$). If A1 is true, then compatibility with the GBH requires furthermore that in the subpopulation of participants showing the *face* effect, (A2) $\Delta\mu_{RT} = 0$ in the *mirrored-face* condition, (A3) $\Delta\mu_{RT} = 0$ or $\Delta\mu_{RT} > 0$ in the *PWC* condition, (A4) $\Delta\mu_{RT} < 0$ in the *horses* condition, and (A5) $\Delta\mu_{RT} < 0$ in the *grating* condition have a higher prevalence than expected by chance. In Q8, we will scrutinize the IBH in the same way by testing (B1) whether the effect of $\Delta\mu_{RT} < 0$ in the *PWC* condition is more frequent than expected by chance. If B1 is true, then we test the prevalence of the following effects to see if they dominate the subpopulation of participants exhibiting $\Delta\mu_{RT} < 0$ in the *PWC* condition: (B2) $\Delta\mu_{RT} < 0$ in the *mirrored-PWC*, (B3) $\Delta\mu_{RT} < 0$ in the *horses*, and (A4) $\Delta\mu_{RT} < 0$ in the *grating* condition. IBH is supported only if all three of the above conditions are fulfilled.

Methods

Ethics information

The research presented here is approved by the Ethics Board of the responsible institution in Germany and is conducted in accordance with the principles of human research ethics of the Declaration of Helsinki. Informed consent is obtained from all participants, and they are compensated with 7€ per half hour.

Design

Our study consists of two parts, a pre-experiment, and the main experiment. Both involve motion-discrimination reaction-time tasks. Researchers are blind to the experimental conditions during data collection. Analysis will not be performed blind.

The pre-experiment consists of 100 trials. In each trial, participants will first see a red central fixation dot (0.5° in diameter) which is shortly after replaced by a random dot motion stimulus (RDMS) with varying noise levels. The movement direction of each individual dot is sampled from a von Mises distribution with a mean of either 90° or 180° (rightwards or leftwards motion, randomized across trials) and varying precision (noise levels). The dots have a lifetime of 200 ms and a velocity of 2 $^\circ$/s. The RDMS is presented in a 5-by-5° square at the center of the screen with black dots on a white background. This procedure generates a flow field with a dominant direction of motion without individual dots representing the respective direction. Participants will be instructed to report the direction as quickly and accurately as possible by pressing the respective button on a button box. Goals of the pre-experiment are to familiarize participants with the discrimination task, and to find the individual noise level defined as the point just before the participants' psychometric function reaches its plateau. Our pilot data suggests that the motion adaptation effect is strongest at this noise level. The individual noise levels will be reported in the *Supplementary* section.

Our main experiment will follow a within-subject design. Participants will have to solve the same motion discrimination task with individually adjusted noise levels preceded by cue images. The cues will either be a sinusoidal grey scale grating moving to the left/right (explained in detail elsewhere[2]) or one out of five different sets of images (referred to as the *cue conditions*). In four of these sets, an image of a tree is presented on one side of the screen, right or left with equal probability, while on the other side, one of the following images appears: *face*, *mirrored-face*, *PWC* and *mirrored-PWC*. Mirrored means that the *face*/*PWC* are facing away from tree. In the fifth one, a single static image of horses, running to right/left selected at random, is presented centrally. Figure 1 illustrates the temporal sequence of a trial as well as the different cue images. The distance between the two images is equal to the width of the RDMS ($\approx 5^{\circ}$). Dimensions of the *PWC* are chosen to match those of the *face* image. In conjunction with the leftwards or rightwards moving dots of the RDMS the cue direction generates *congruent* and *incongruent* trials. Cue direction is defined as *towards the tree*, running direction of the horses, and movement direction of the grating. For example, if the tree is on the left side and the *mirrored-face* or the *face* on the right, in both cases the cue direction is defined as leftwards. This avoids conflicts when it comes to the IBH and the *PWC* stimulus. The central fixation dot will be presented for 1.5 s, followed by the cue that lasts 1.5 s. As soon as the RDMS appears, participants will have 2s to report its direction of motion. In the design of the *face* images, the moving grating, and RDMS as well as the temporal sequence and duration of presentation of stimuli, we will replicate the specifications detailed in Guterstam *et al.*[2]. We will deviate from Guterstam et al. in the algorithm with which we generate the RDMS. We draw the motion directions of individual dots from a von Mises distribution while they had a subset of dots moving in the respective direction. Our method has the advantage that it prohibits the strategy to use individual dots to identify the motion direction. Further, Guterstam et al. used a fixed noise level for all participants and excluded those who did not achieve 80 % accuracy. We on the other hand will adapt the noise level to participants individual capabilities.

Each run will contain 50-60 trials of a maximum of three different *cue-conditions*. Within each run, trials of each cue and congruency condition are randomly interleaved and counterbalanced. To eliminate the influence of a strong motion aftereffect elicited by the moving grating on the performance in other cue conditions in subsequent trials, the moving grating will be tested in separate runs only. We limit the number of conditions within each run to mitigate the effect of outlier RTs as we include *run* as group-level effect in our regression model. Participants will perform the mirrored conditions of the *face* and *PWC* stimuli only if they show a difference between the RTs of congruent and incongruent conditions in the non-mirrored variants.

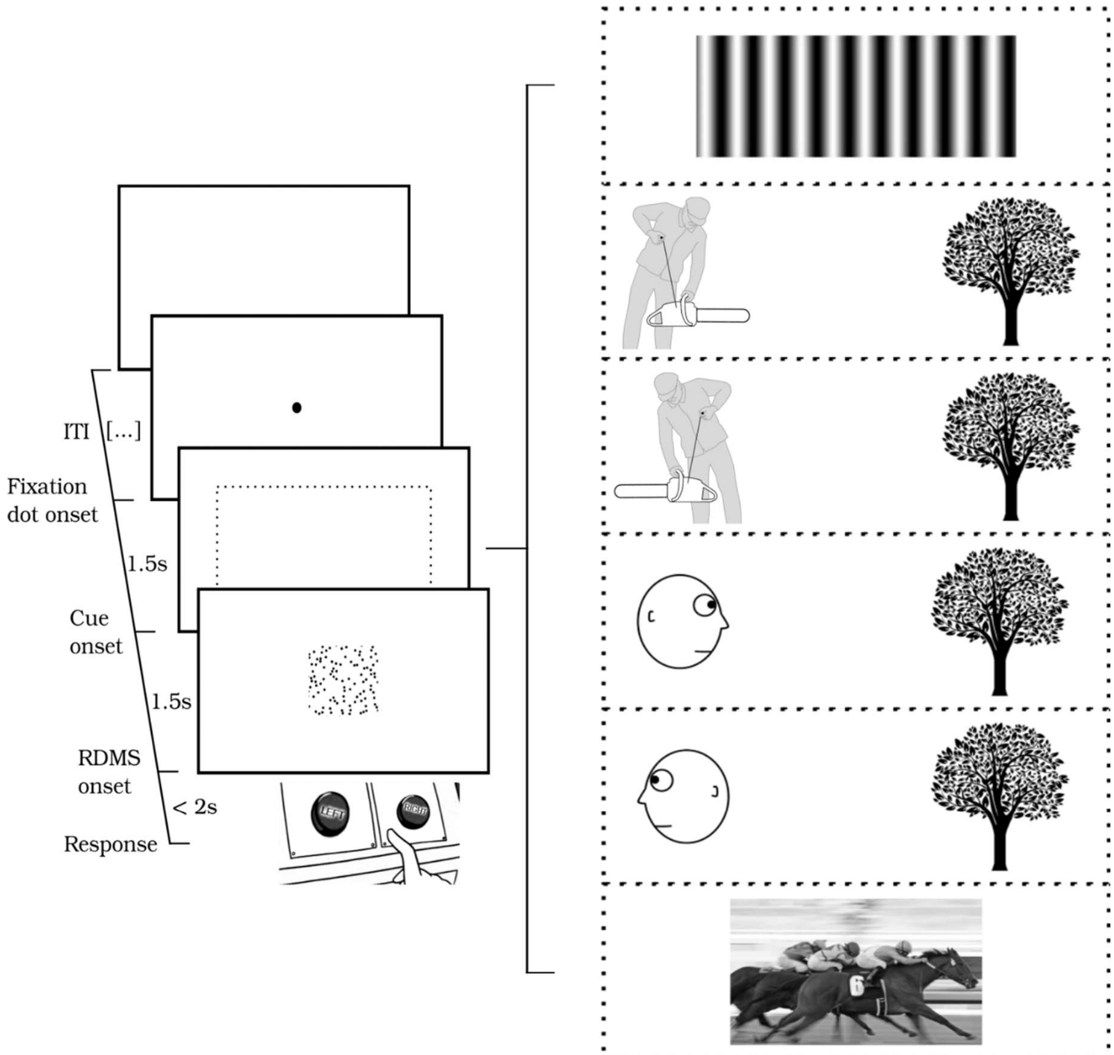

Figure 1. Illustration of the paradigm. Left side shows the temporal sequence of trial events. Right side depicts the stimuli in the various cue conditions as well as in the grating condition.

Sampling plan

The first part of the analysis will be conducted at the participant level reaction times, i.e., each participant's data is analyzed individually for differences between RT_c and RT_{ic} trials. The second part will deal with the distribution of individual effects (RT_c smaller, larger, or equal to RT_{ic}) within the population of participants. According to the guidelines of Bayesian hypothesis testing, we will collect data until all computed Bayes Factors (BFs) concerning reaction times as well as effect distributions are at least 10 in favour of the null or the alternative hypotheses. This means that we collect data from each participant and add further participants to the population for the analysis of effect distributions until this criterion is reached or the number of participants exceeds 35 chosen due to practical reasons. Pilot experiments suggest that each participant must complete 150-400 trials per condition. If the BF associated to any of the cue-conditions does not reach the threshold within 750 trials, data collection from the corresponding participant will cease. This limit of 750 trials is chosen for practical reasons. Since we are not able to analyze the data after each run during an on-going experiment but only after a completed session, we will accept the BF requirement being met if during the session there is a run with a BF crossing the threshold. To be fully transparent in this regard we will conduct an sequential analysis to check the development of the BFs as a function of runs. These will be reported in the supplementary data section. Since participants have the right to drop out of the experiment at any time, we might encounter situations in which the BF for one or the other cue condition is outside the target range. In such scenarios, the BFs will not be included in the population-level data analysis.

Regarding the population-level analysis of the effect distributions, simulations show that, in the best case, no more than 5 participants will be required (calculated using the Bayesian Binomial test described below). Within cue-conditions, we group participant-level BFs into two categories: moderate/strong evidence ($BF_{01} > 3$ or $BF_{01} < 1/3$), and strong evidence ($BF_{01} > 10$ or $BF_{01} < 1/10$). Population data analysis will be performed for each category separately.

Analysis Plan

Analysis is based on trials with correct responses only. No further outlier removal is performed.

Differences in reaction time and its variance at the participant level

We are interested in the effect of the congruency-condition grouped by cue-condition on reaction times. RTs will be analyzed for each participant individually. To this end, for each cue-condition we will fit (distributional) Bayesian hierarchical models with congruency condition as the population-level/ fixed effect and runs as group-level/ random intercepts and slopes (*brms*[18]-notation:

```
bf(
    RT | trunc(ub = 2000) ~ congruency-condition + (congruency-condition || Run),
    sigma | trunc(ub = 2000) ~ congruency-condition + (congruency-condition || Run),
    family = shiσfted_lognormal(link = "identity")).
```

We will use congruency-condition not only as a predictor for the mean but also for the variance since pilot data suggested that effects on the variance exist as well. The outcome variable is truncated at an upper bound of 2000 ms reflecting the maximum RTs allowed by the experimental design. Runs will only be included as group-level factors, *(MotionCongruency || Run),* if the number of runs is larger than 5 as suggested by Bolker[17]. Priors for the outcome variables are tuned such that prior and posterior predictive checks yield reasonable results for the pilot data and simulated data. The following priors outcome variables *RT* and *sigma* will be used:

$$\text{Intercept}(\mu_{RT}) \sim N(5, 0.5)$$
$$\text{sd}(\mu_{RT}) \sim N(0.02, 0.05) \text{ with lower bound} = 0$$
$$ndt \sim N(200, 70) \text{ with lower bound} = 100$$

and

$$\text{Intercept}(\sigma_{RT}) \sim N(-1, 0.2)$$
$$\text{sd}(\sigma_{RT}) \sim N(0.3, 0.5) \text{ with lower bound} = 0.$$

Intercept(μ_{RT}/σ_{RT}) represents the RT/variance in the *congruent* condition, sd(μ_{RT}/σ_{RT}) the variance across runs and *ndt* is a parameter that represents the shift of the log-normal distribution away from 0. As priors for the effects of congruency-condition on the parameters of interest, the difference between the RTs/variances in the congruent and incongruent condition, we will use:

$$\Delta\mu_{RT} \sim N(0, 0.2)$$
$$\Delta\sigma_{RT} \sim N(0, 0.3)$$

These priors are weakly informative in the sense that we expect an effect within a range of ±0.25 which is the range where this prior has roughly 80% of its mass. Mind that all values but the values for *ndt* reported here are on the model internal log-scale which incorporates the estimate for *ndt*.

We will compute BFs for the point-Null-hypotheses specified in Table 1 using the Savage-Dickey[19] approach which computes BFs as the ratio between the posterior and the prior distributions at the specified parameter value, here 0. This procedure is equivalent to a two-sided test. The model is run using the standard settings of *brms* (4 Markov chains with 2000 iterations, each). In addition to the BFs, we will report the estimates for $\Delta\mu_{RT}$ and their 95% Credible Intervals. For better understanding, the estimates for $\Delta\mu_{RT}$ will be transformed into *ms* using the formula $e^{\text{Intercept}(\mu_{RT})+\Delta\mu_{RT}} - e^{\text{Intercept}(\mu_{RT})}$.

Testing the validity of GBH and IBH at the population level

To test whether any of the two hypotheses is supported at the population level, we will analyse the distribution of effects. This will be done by computing BFs using a Bayesian Binomial test with the test value p_0 set to $^1/_3$, the chance level of observing a specific effect. For the GBH to be supported, first, the prevalence of the effect of $\Delta\mu_{RT} < 0$ in the *face* condition must be higher than p_0 (A1). Second, If A1 is true, then the following further requirements must be met by the subpopulation showing the effect: (A2) the fraction with $\Delta\mu_{RT} = 0$ in the *mirrored-face* condition dominates, (A3) the fraction with $\Delta\mu_{RT} < 0$ in the *PWC* condition is smaller or equal to chance, (A4) the fraction with $\Delta\mu_{RT} < 0$ in the *horses* condition dominates, and (A5) the fraction with $\Delta\mu_{RT} < 0$ in the *grating* condition dominates. Conditions A2 to A5 are tested by the same type of Binomial test as A1.

For IBH to be supported at the population level, (B1) the fraction of participants with $\Delta\mu_{RT} < 0$ in the *PWC* condition must be higher than p_0. Plus, in the subpopulation showing $\Delta\mu_{RT} < 0$ in the *PWC* condition, (B2) the fraction with $\Delta\mu_{RT} < 0$ in the *mirrored-PWC* condition, (B2) the fraction with $\Delta\mu_{RT} < 0$ in the *horses* condition, and lastly, (B4) the fraction with $\Delta\mu_{RT} < 0$ in the *grating* condition must be larger than p_0.

All analyses are conducted using custom-made scripts in Matlab[20], and R[21]. For Bayesian modelling and hypothesis testing, the R package *brms*[18] (individual RTs) and JASP[22] (effect distributions) are used. Tests concerning individual RTs will be two-sided, Binomial tests concerning effect distributions one-sided.

Timeline

We estimate that we will complete the study within three months from the date we receive a successful Stage 1 review.

Pilot data

We collected pilot data from two subjects until all Bayes Factors exceeded the evidence threshold. Pilot subject 2 was not subjected to the mirrored variants of the *PWC* and the *face* stimulus since in case of this subject the respective *null*-hypotheses of $\Delta\mu_{RT} = 0$ were favored over the alternatives.

Both subjects showed a motion adaptation effect for the grating condition. In all other conditions but the *mirrored-face* condition, pilot subject 1 showed response priming effects, i.e. $\Delta\mu_{RT} > 0$. The data of pilot subject 2 provided evidence in favor of the respective *null*-hypotheses. Bayes Factors and effect estimates are shown in Table 2. The respective RT distributions are shown in Supplementary Figure 1.

Table 2. Pilot subjects' results of all conditions

	Pilot subject 1		**Pilot subject 2**	
	$\mathbf{log_{10}(BF_{01})}$	$\Delta\mu_{RT}$, **[l-CI, u-CI]**	$\mathbf{log_{10}(BF_{01})}$	$\Delta\mu_{RT}$, **[l-CI, u-CI]**
PWC	-4.62	0.04, [0.02, 0.05]	1.04	0.00, [-0.02, 0.04]
Mirrored-PWC	-1.47	0.02, [0.01, 0.03]	-	-
face	-1.6	0.02, [0.01, 0.03]	1.04	-0.01, [-0.02, 0.01]
Mirrored-face	1.18	0.00, [-0.01, 0.01]	-	-
Grating	-11.96	-0.03, [-0.05, -0.02]	-31.72	-0.09, [-0.12, -0.07]
horses	-1.1	0.02, [0.01, 0.03]	1.15	0.00, [-0.02, 0.02]

l-CI and u-CI are the lower and upper boundaries of the 95% Credible Interval of the estimate. $\Delta\mu_{RT}$ is given in seconds. Bayes Factors are given from the perspective of the *null*-hypothesis, $\Delta\mu_{RT} = 0$ (see Table 2).

References

1. Guterstam, A., Kean, H. H., Webb, T. W., Kean, F. S. & Graziano, M. S. A. Implicit model of other people's visual attention as an invisible, force-carrying beam projecting from the eyes. *Proceedings of the National Academy of Sciences of the United States of America* **116**, 328–333 (2019).
2. Guterstam, A. & Graziano, M. S. A. Implied motion as a possible mechanism for encoding other people's attention. *Progress in Neurobiology* 101797 (2020) doi:10.1016/j.pneurobio.2020.101797.
3. Guterstam, A., Wilterson, A. I., Wachtell, D. & Graziano, M. S. A. Other people's gaze encoded as implied motion in the human brain. *PNAS* (2020) doi:10.1073/pnas.2003110117.
4. Guterstam, A. & Graziano, M. S. A. Visual motion assists in social cognition. *Proceedings of the National Academy of Sciences* **117**, 32165–32168 (2020).
5. Kourtzi, Z. & Kanwisher, N. Activation in Human MT/MST by Static Images with Implied Motion. *Journal of Cognitive Neuroscience* **12**, 48–55 (2000).
6. Winawer, J., Huk, A. C. & Boroditsky, L. A motion aftereffect from still photographs depicting motion. *Psychological science* **19**, 276–83 (2008).
7. Faivre, N. & Koch, C. Inferring the direction of implied motion depends on visual awareness. *Journal of Vision* **14**, 4–4 (2014).
8. Görner, M., Ramezanpour, H., Chong, I. & Thier, P. Does the brain encode the gaze of others as beams emitted by their eyes? *Proceedings of the National Academy of Sciences of the United States of America* **117**, 20375–20376 (2020).
9. Shulman, G. L. *et al.* Areas Involved in Encoding and Applying Directional Expectations to Moving Objects. *Journal of Neuroscience* **19**, 9480–9496 (1999).
10. Luks, T. L. & Simpson, G. V. Preparatory deployment of attention to motion activates higher-order motion-processing brain regions. *NeuroImage* **22**, 1515–1522 (2004).
11. Premack, D. & Woodruff, G. Does the chimpanzee have a theory of mind? *Behavioral and Brain Sciences* **1**, 515–526 (1978).

12. Schlack, A. & Albright, T. D. Remembering Visual Motion: Neural Correlates of Associative Plasticity and Motion Recall in Cortical Area MT. *Neuron* **53**, 881–890 (2007).

13. Cheong, D., Zubieta, J.-K. & Liu, J. Neural Correlates of Visual Motion Prediction. *PLoS One* **7**, (2012).

14. Wurm, M. F. & Caramazza, A. Two 'what' pathways for action and object recognition. *Trends in Cognitive Sciences* (2021) doi:10.1016/j.tics.2021.10.003.

15. Klotz, W. & Neumann, O. Motor activation without conscious discrimination in metacontrast masking. *Journal of Experimental Psychology: Human Perception and Performance* **25**, 976–992 (1999).

16. Campana, G., Cowey, A. & Walsh, V. Priming of Motion Direction and Area V5/MT: a Test of Perceptual Memory. *Cereb Cortex* **12**, 663–669 (2002).

17. Bolker, B. *GLMM FAQ*. http://bbolker.github.io/mixedmodels-misc/glmmFAQ.html.

18. Bürkner, P.-C. brms: An R Package for Bayesian Multilevel Models Using Stan. *Journal of Statistical Software* **80**, 1–28 (2017).

19. Faulkenberry, T. J. Savage-Dickey Density Ratio for computing Bayes Factors. *The Book of Statistical Proofs* https://statproofbook.github.io/P/bf-sddr.html (2020).

20. MATLAB. 9.7.0.1190202 (R2021a). (The MathWorks Inc. 2018).

21. R Core Team. R: A Language and Environment for Statistical Computing. (2021).

22. JASP Team. JASP2022. (2022).

Data availability statement:

The data that support the findings of this study will be openly available under https://osf.io/gh76s/ including pilot data.

Acknowledgements:

We thank Dr. Friedemann Bunjes and Peter W. Dicke for their invaluable technical assistance.

Table 1. Design table: Hypotheses are formulated to fit our model specifications.

Question	Hypothesis	Sampling plan	Analysis Plan	Interpretation
		Participant level analysis		
Q1. Grating *(control 1)*: Can we reproduce the standard motion adaptation effect?	$H_{0,1}$: $\Delta\mu_{RT} = 0$	$\mathrm{BF} \geq 10$	Bayesian hierarchical model	If a participant does not yield $\Delta\mu_{RT} < 0$, i.e., faster RT in the incongruent condition then our setup is not capable to induce/ capturing the motion adaptation effect for that participant (cf. *Q7*).
Q2. Horses *(control 2)*: Does the applied method allow an *implied motion* stimulus to elicit motion adaptation?	$H_{0,2}$: $\Delta\mu_{RT} = 0$	$\mathrm{BF} \geq 10$	Bayesian hierarchical model	If $\Delta\mu_{RT} < 0$ then our setup is capable of inducing motion adaptation via an implied motion stimulus. Required to interpret a congruent effect in *Q3* in terms of motion adaptation. $\Delta\mu_{RT} = 0$ or $\Delta\mu_{RT} > 0$ means evidence that our setup is not capable of inducing motion adaptation via an implied motion stimulus. In the limits of the replication of Guterstam and colleagues' method this result is evidence against the gaze-beam hypothesis independent of the outcome of

				Q3. $\Delta\mu_{RT}$ > 0 will be interpreted such that the stimulus induces response priming.
Q3. Face *(replication)*: Can we replicate the *face-effect* as reported by Guterstam and colleagues[2,3]?	$H_{0,3}$: $\Delta\mu_{RT} = 0$	$\mathrm{BF} \geq 10$	Bayesian hierarchical model	$\Delta\mu_{RT}$ < 0 provides evidence in favor of Guterstam's et al. gaze-beam hypothesis [2,3]. If the result is in favour of $\Delta\mu_{RT}$ = 0 or $\Delta\mu_{RT}$ > 0 then the results from Guterstam and colleagues[2] are not reproduced, i.e., there is no effect or an effect inverse to what is expected if motion adaptation is the underlying mechanism. In case of $\Delta\mu_{RT}$ > 0, a priming effect is the suggested alternative explanation.
Q4. face mirrored *(replication)*: Control for orientation specificity of potential effects observed in *Q3*[2,3]?	$H_{0,4}$: $\Delta\mu_{RT} = 0$	$\mathrm{BF} \geq 10$	Bayesian hierarchical model	Results will be interpreted in conjunction with *Q3* to control orientation specificity.
Q5. Person-with-chainsaw:	$H_{0,5}$: $\Delta\mu_{RT} = 0$	$\mathrm{BF} \geq 10$	Bayesian hierarchical model	$\Delta\mu_{RT}$ < 0 will be interpreted such that the stimulus induces motion adaptation.

Does a cue that contains some intentional/ causal binding between an agent and an object elicit an effect?				$\Delta\mu_{RT}$ > 0 will be interpreted such that the stimulus induces response priming.
Q6. Person-with-chainsaw mirrored: Control for orientation specificity of potential effects observed in *Q5*.	$H_{0,6}$: $\Delta\mu_{RT} = 0$	$\mathrm{BF} \geq 10$	Bayesian hierarchical model	Results will be interpreted in conjunction with *Q5* to control orientation specificity.
Population level analysis				
Q7*.* Is there evidence for GBH at the population level?	$H_{0,\mathrm{A}1}: \frac{\#(\Delta\mu_{RT_{face}} < 0)}{\#\mathrm{Participants}} \leq 1/3$ $H_{0,\mathrm{A}2}: \frac{\#(\Delta\mu_{RT_{mirrored\text{-}face}} = 0)}{\#\mathrm{Participants}(\Delta\mu_{RT_{face}} < 0)} \leq 1/3$ $H_{0,\mathrm{A}3}: \frac{\#(\Delta\mu_{RT_{PWC}} < 0)}{\#\mathrm{Participants}(\Delta\mu_{RT_{face}} < 0)} \geq 1/3$ $H_{0,\mathrm{A}4}: \frac{\#(\Delta\mu_{RT_{horses}} < 0)}{\#\mathrm{Participants}(\Delta\mu_{RT_{face}} < 0)} \leq 1/3$	$\mathrm{BF} \geq 10$ or #Participants < 35	Bayesian Binomial Test with test value $p_0 = {}^{1}/_{3}$.	Population level GBH is supported if we find evidence in favour of $H_{1,\mathrm{A}1}$, $H_{1,\mathrm{A}2}$, $H_{1,\mathrm{A}3}$, $H_{1,\mathrm{A}4}$ and $H_{1,\mathrm{A}5}$. If we find deviating evidence for any of these GBH will be rejected at the population level.

	$H_{0,\mathrm{A5}}\colon \frac{\#(\Delta\mu_{RT_{grating}} < 0)}{\#\mathrm{Participants}(\Delta\mu_{RT_{face}} < 0)} \leq 1/3$ *$\#\mathrm{Participants}(\Delta\mu_{RT_{face}} < 0)$ denotes the subpopulation of participants showing the effect of $\Delta\mu_{RT_{face}} < 0$.			
***Q8**. Is there evidence for IBH on the population level?*	$H_{0,\mathrm{B1}}\colon \frac{\#(\Delta\mu_{RT_{PWC}} < 0)}{\#\mathrm{Participants}} \leq 1/3$ $H_{0,\mathrm{B2}}\colon \frac{\#(\Delta\mu_{RT_{mirrored\text{-}PWC}} < 0)}{\#\mathrm{Participants}(\Delta\mu_{RT_{PWC}} < 0)} \leq 1/3$ $H_{0,\mathrm{B3}}\colon \frac{\#(\Delta\mu_{RT_{horses}} < 0)}{\#\mathrm{Participants}(\Delta\mu_{RT_{PWC}} < 0)} \leq 1/3$ $H_{0,\mathrm{B4}}\colon \frac{\#(\Delta\mu_{RT_{grating}} < 0)}{\#\mathrm{Participants}(\Delta\mu_{RT_{PWC}} < 0)} \leq 1/3$	$\mathrm{BF} \geq 10$ or #Participants < 35	Bayesian Binomial Test with test value $p_0 = {}^1/_3$.	Population level IBH is supported if we find evidence in favour of $H_{1,B1}$, $H_{1,B2}$, $H_{1,B3}$ and $H_{1,B4}$. If we find deviating evidence for any of these IBH will be rejected at the population level

Supplementary materials

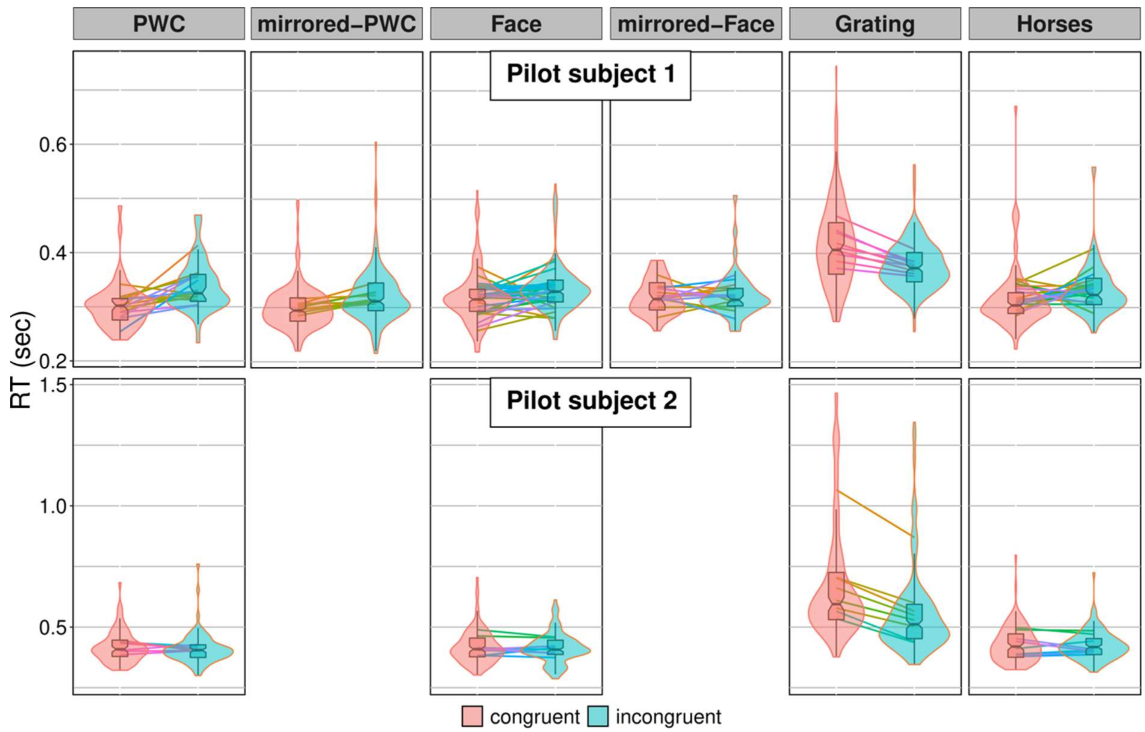

Supplementary Figure 1: Plots show the RT-distributions for all conditions and both pilot subjects grouped by congruency condition. Lines represent individual runs.